Acousto-optic Q-switched laser performances of Er^{3+}:Yb^{3+}:$LuAl_3(BO_3)_4$ crystal at 1.5–1.6 μm

Yujin Chen (陈雨金)[1], Yanfu Lin (林炎富)[1], Haiyong Zhu (朱海永)[2], Ge Zhang (张 戈)[1], and Yidong Huang (黄艺东)[1*]

[1] *Key Laboratory of Optoelectronic Materials Chemistry and Physics, Fujian Institute of Research on the Structure of Matter, Chinese Academy of Sciences, Fuzhou 350002, China*

[2] *College of Physics and Electronic Information, Wenzhou University, Wenzhou 325035, China*

[*] *Corresponding author: huyd@fjirsm.ac.cn*

Received May 18, 2011; accepted July 25, 2011; posted online September 22, 2011

Diode-pumped acousto-optic Q-switched pulse laser at 1.5–1.6 μm is obtained in an Er^{3+}:Yb^{3+}:$LuAl_3(BO_3)_4$ crystal. Single-pulse laser operation with slope efficiency of 14% and threshold of approximately 100 mW is realized at an average absorbed pump power of 314 mW and repetition frequency of 20 kHz. Output pulse energy is 67 μJ. The effects of pulse repetition frequency, absorbed pump power, and duty cycle on the wavelength and pulse profile of the Q-switched Er^{3+}:Yb^{3+}:$LuAl_3(BO_3)_4$ laser are also investigated.

OCIS codes: 140.3500, 140.3480, 140.3540.
doi: 10.3788/COL201210.021403.

Q-switched pulse laser at 1.5–1.6 μm with high repetition frequency has applications in numerous fields, including range finding, lidar, and telecommunications. Compared with passively Q-switched pulse laser, actively Q-switched laser has smaller interpulse time jittering and more stable pulse repetition frequency (PRF)[1]. Therefore, actively Q-switched pulse laser is more suitable for several applications. Er^{3+} and Yb^{3+} co-doped phosphate glass, which at present is the most well-known 1.5–1.6-μm gain medium[2−5], is limited by its low thermal conductivity. Thus, it is rendered ineffective in attaining the Q-switched pulse laser with high performance. Crystalline materials with higher thermal conductivity are appropriate alternatives for the Q-switched laser operation[6].

Numerous investigations have shown that Er^{3+}/Yb^{3+} co-doped borate crystals with high effective phonon energy of approximately 1400 cm^{-1} are one of the ideal gain media for the 1.5–1.6-μm laser[6−12]. Important spectroscopic parameters and thermal conductivities of Er^{3+}/Yb^{3+} co-doped $LuAl_3(BO_3)_4$ (LuAB), $YAl_3(BO_3)_4$ (YAB), $YCa_4O(BO_3)_3$ (YCOB), and $GdCa_4O(BO_3)_3$ (GdCOB) crystals are listed in Table 1. The spectroscopic parameters of Er:Yb:LuAB crystal are similar to those of Er:Yb:YAB crystal. Except for the shorter fluorescence lifetime of $^4I_{13/2}$ upper lasing state of Er^{3+} ions, the other parameters of Er:Yb:LuAB crystal are superior to those of Er^{3+}/Yb^{3+} co-doped YCOB and GdCOB crystals. Furthermore, related investigation has determined that the thermal performance of LuAB crystal should be similar to that of YAB crystal[13] and thus, superior to those of YCOB and GdCOB crystals. At present, continuous-wave (CW) laser with slope efficiency of up to 35% and passively mode-locked laser with pulse duration of 3.8 ps have been realized in Er:Yb:YAB crystals[9,14]. Er:Yb:LuAB crystal has higher optical quality and better CW laser performance than those of the Er:Yb:YAB crystal because the radius and mass of Lu^{3+} ion are closest to those of Yb^{3+} ion[7]. In this letter, actively Q-switched laser performances in an Er:Yb:LuAB crystal are reported. Furthermore, the relation between output laser wavelength and pulse characteristic is investigated in detail.

Table 1. Important Spectroscopic Parameters and Thermal Conductivities of Er^{3+}/Yb^{3+} Co-doped LuAB, YAB, YCOB, and GdCOB Crystals

Parameter	LuAB[7]	YAB[8,9]	YCOB[10,11]	GdCOB[6,12]
Absorption Wavelength λ_p	976	976	976	976
FWHM at λ_p	19	19	3	3
Absorption Cross Section at λ_p ($\times 10^{-20}$ cm^2)	3.3	3.1	0.9	1.1
Gain Cross Section at Laser Wavelength (β=0.5) ($\times 10^{-20}$ cm^2) (nm)	0.23 1 598	0.2 1 598	0.1 1 545	
Lifetime of $^4I_{13/2}$ Upper Lasing State of Er^{3+} (ms)	0.31 (1.1 at.-% Er^{3+})	0.32 (1.5 at.-% Er^{3+})	1.26 (2.0 at.-% Er^{3+})	1.2 (2.5 at.-% Er^{3+})
Thermal Conductivity ($W \cdot m^{-1} \cdot K^{-1}$)		4.7	2.65	2.4

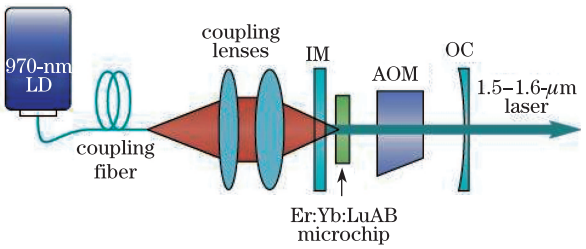

Fig. 1. Experimental setup of the quasi-CW diode-pumped acousto-optic Q-switched Er:Yb:LuAB laser.

A c-cut, 0.7-mm-thick Er (1.1 at.-%):Yb (24.1 at.-%):LuAB microchip was used as gain medium and an end-pumped linear resonator was adopted in the experiment. The experimental setup is shown in Fig. 1. A 970-nm fiber-coupled laser diode (LD) (800-μm-diameter core) (Coherent Inc.) was used as pump source. After passing a simple coupling lens system, the pump beam was focused to a spot in the microchip which has a waist diameter of approximately 290 μm. The uncoated sample was attached to an aluminum slab with heat-conducting adhesive. A hole at the center of the slab permits the passing of the pump and fundamental laser beams. No other device was used to control the cooling of the microchip. Thus, the LD was operated in the quasi-CW mode to reduce the influence of the pump-induced thermal load on the laser performance and prevent fracture of the microchip at high pump power. The pump pulse width was 2 ms and the pulse period was 100 ms. The σ-polarized absorption coefficient of the Er:Yb:LuAB crystal is approximately 29 cm^{-1} at the pump wavelength of 970 nm[7]. Subsequently, approximately 85% of incident pump power is absorbed by the microchip. The flat input mirror (IM) achieves 90% transmission at 970 nm and 99.8% reflectivity at 1.5–1.6 μm. The transmission of the output coupler (OC) with 50-mm radius of curvature (RoC) is 1.5% at 1.5–1.6 μm. The cavity length was set near to the RoC of the OC. In order to realize actively Q-switched operation, an acousto-optic modulator (AOM) (Gooch & Housego Co.) with antireflection coated at 1.5–1.6 μm and driven at 80 MHz center frequency with 10 W of radio-frequency power was inserted between the microchip and OC. With good alignment of AOM, lasing can be effectively prohibited when the radio-frequency signal is supplied and Q-switching takes place when the radio-frequency signal is switched off. The pulse profile was measured by a 2-GHz InGaAs photodiode connected to a digital oscilloscope with bandwidth of 1 GHz (DSO6102A, Agilent). The laser spectrum was recorded with a monochromator (Triax550, Jobin-Yvon) in combination with a TE-cooled Ge detector (DSS-G025T, Jobin-Yvon).

Previous experiment has shown that higher peak power and narrower pulse width of Q-switched laser can be obtained when the modulator has a lower duty cycle (DC)[15] which is defined as the ratio of the cavity opening time to the cavity modulation period. Therefore, the necessity of exploring a suitable DC of modulator for enhancing the pulse laser performance should be the primary consideration. The average output powers of the Q-switched Er:Yb:LuAB laser were measured for various DCs and PRFs of AOM. For brevity, Fig. 2 only shows the experimental result when PRF is 20 kHz. For both the average absorbed pump powers of 314 and 196 mW, average output power increases rapidly under low DC. Subsequently, a tendency toward saturation is shown with the increment of DC. Furthermore, when a high DC was used, the cavity opening required a long period of time such that the laser system operated in both CW and Q-switched modes. Therefore, to achieve pulse laser with higher performance, the DC indicated by the dashed line in Fig. 2 was adopted. The inset in Fig. 2 shows the adopted DCs at various PRFs. The values are 0.6%, 1.2%, 4%, 7%, 12%, and 15% when the PRFs are 3, 5, 10, 20, 40, and 60 kHz, respectively. For these adopted DCs, the cavity opening time is short enough (approximately 2-4 μs). This can facilitate generation of highly efficient Q-switched pulse within the short time. In addition, the effect of the CW-background can be neglected[1]. The PRFs used are higher than 3 kHz. This shows that the pump durations between adjacent output pulses are shorter than the lifetime (0.3 ms) of $^4I_{13/2}$ upper lasing state of Er^{3+} ions. Under this situation, wasting of pump energy is prevented. Furthermore, the short upper lasing state lifetime of Er:Yb:LuAB crystal may decrease the energy storage capability, as well as the extraction efficiency and output pulse energy[16].

Figure 3 shows the spectra and pulse profiles of the Q-switched Er:Yb:LuAB laser for different PRFs at an average absorbed pump power of 314 mW and corresponding adopted DC. When PRF is lower than 20 kHz, the output laser is multi-wavelength and the profile is pulse-bunch. At PRF of 3 kHz, the width of the first spike of the pulse-bunch is only 35 ns. When PRF is higher than 20 kHz, the output laser is single-wavelength and the profile is single-pulse. Furthermore, with the reduction of PRF, the laser output power gradually flows from the long wavelength to the short one and the width of the first spike becomes narrower. When PRF decreases, the initial population inversion density and the gain of Q-switched laser increase[16] which causes the blue shift of laser wavelength[7,8] and the narrowing of pulse width[17]. At the same time, higher initial population inversion density of the Q-switched laser with lower PRF enhances the populations on higher crystal field levels of the $^4I_{13/2}$ multiplet. These levels correspond

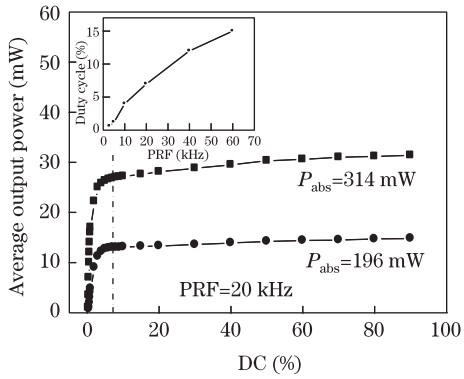

Fig. 2. Average output powers of the Q-switched Er:Yb:LuAB laser at different DCs and average absorbed pump powers when the PRFs is 20 kHz. The inset shows the adopted DCs in the experiment at different PRFs.

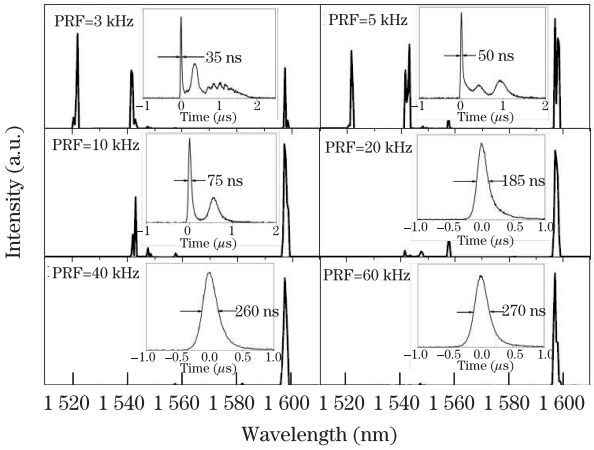

Fig. 3. Spectra and pulse profiles of the Q-switched Er:Yb:LuAB laser for different PRFs at average absorbed pump power of 314 mW and corresponding adopted DC.

to the upper sub-levels of the transitions with shorter wavelengths[18,19]. Consequently, the increase of the gain at these transitions leads to the multi-wavelength laser oscillation[7,8] where the different transition characteristics of these lasers may cause the generation of the pulse-bunch profile[20].

For different PRFs at the corresponding adopted DC, average output powers of the Q-switched Er:Yb:LuAB laser were measured. The results are shown in Fig. 4. When PRF decreases from 60 to 3 kHz at the maximum average absorbed pump power of 314 mW, the average output power and the slope efficiency decreases from 29 to 10 mW and from 15.5% to 4.8%, respectively. The laser threshold is approximately 100 mW. When the quasi-CW pump light with pulse width of 2 ms and period of 100 ms was taken into account, the calculated pulse energy increases from 24.2 to 167 μJ. At this particular phase of the pulse-bunch operation, the pulse energy is the total energy of a pulse-bunch profile[21]. The obtained maximum energy of the acousto-optic Q-switched Er:Yb:LuAB laser is relatively higher than those reported previously for the acousto-optic Q-switched Er:Yb:YAB crystal (91 μJ)[22], acousto-optic Q-switched Er:Yb:phosphate glass (12 μJ)[1], and passively Q-switched Er:Yb:GdCOB crystal (approximately 3 μJ) lasers[6]. The value is comparable to that of mechanical Q-switched Er:Yb:YVO_4 (approximately 0.2 mJ) laser[23]. Because of the pulse-bunch operation of Q-switched Er:Yb:LuAB laser for PRF lower than 20 kHz, the peak power cannot be estimated. For the single-pulse operation at PRF of 20 kHz, the pulse energy is 67 μJ and the peak power is approximately 362 W according to the pulse width of 185 ns as shown in Fig. 3. The experimental results of the acousto-optic Q-switched Er:Yb:LuAB laser are summarized in Table 2. It must be pointed out that the Er:Yb:LuAB microchip used in this work was not antireflection coated. Thus, in future studies, antireflection coating should be deposited on the Er:Yb:LuAB microchip. Coupled with the optimized transmission of the OC, this can possibly achieve the pulse with the higher output energy and efficiency.

Table 2. Experimental Results of the Acousto-optic Q-switched Er:Yb:LuAB Laser

PRF (kHz)	Adopted DC (%)	Maximum Average Output Power (mW)	Slope Efficiency (%)	Pulse Profile	Pulse Energy (μJ)	Pulse Width (ns)	Peak Power (W)
3	0.6	10	4.8	Pulse-bunch	167		
5	1.2	15	7	Pulse-bunch	150		
10	4	23	11.4	Pulse-bunch	115		
20	7	26.6	14	Single-pulse	67	185	362
40	12	28.5	15.3	Single-pulse	36	260	138
60	15	29	15.5	Single-pulse	24.2	270	90

The effects of different absorbed pump powers and DCs on the pulse characteristics of the Q-switched Er:Yb:LuAB laser were also investigated. In Fig. 5, the spectra and pulse profiles of the Q-switched Er:Yb:LuAB laser for different average absorbed pump powers at DC of 0.6% when PRF is 3 kHz are shown. Figure 6 presents the different DCs at the average absorbed pump power of 314 mW. Figure 5 demonstrates that with the reduction of average absorbed pump power, the output power gradually flows from the short wavelength to the long one and pulse profile changes from pulse-bunch to single-pulse. At the average absorbed pump power of 158 mW, single-wavelength oscillation around 1 600 nm and a single-pulse profile with width of 155 ns are obtained. The same trend is also observed in the increase of DC, as shown in Fig. 6. When DC is 80%, single-wavelength oscillation around 1 600 nm and single-pulse

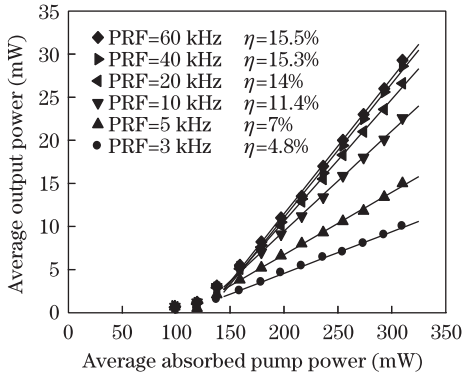

Fig. 4. Average output power versus average absorbed pump power of the Q-switched Er:Yb:LuAB laser for different PRFs at the corresponding adopted DC.

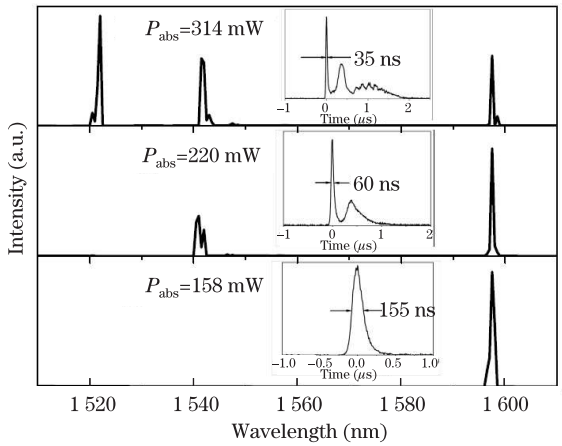

Fig. 5. Spectra and pulse profiles of the Q-switched Er:Yb:LuAB laser for different average absorbed pump powers when PRFs is 3 kHz and DC is 0.6%.

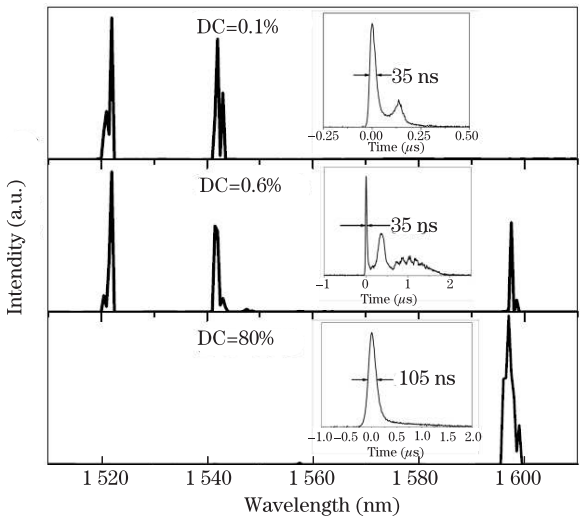

Fig. 6. Spectra and pulse profiles of the Q-switched Er:Yb:LuAB laser for different DCs when PRF is 3 kHz and average absorbed pump power is 314 mW.

profile with width of 105 ns are obtained. However, both CW and Q-switched modes were observed in this case. For the lower absorbed pump power and larger DC, which implies longer cavity opening time, the realization of single-wavelength laser with single-pulse profile can also be explained by the reduction of initial population inversion density.

In conclusion, acousto-optic Q-switched pulse laser performances are investigated for a c-cut, 0.7-mm-thick Er:Yb:LuAB microchip in a diode end-pumped hemispherical cavity. At the average absorbed pump power of 314 mW and PRF of 20 kHz, single-pulse laser operation with slope efficiency of 14% and threshold of approximately 100 mW is realized with the corresponding pulse energy of 67 μJ, pulse width of 185 ns, and peak power of 362 W, respectively. When PRF and DC decrease and absorbed pump power increases, the output power gradually flows from the long wavelength to the short one and pulse width decreases. Meanwhile, the generation of pulse-bunch accompanied by the multi-wavelength oscillation is observed in the Q-switched laser with low PRF.

This work was supported by the National Natural Science Foundation of China (No. 50802094) and the Knowledge Innovation Program of the Chinese Academy of Sciences (No. KJCX2-EW-H03-01).

References

1. G. Karlsson, V. Pasiskevicius, F. Laurell, and J. A. Tellefsen, Opt. Commun. **217,** 317 (2003).
2. P. Laporta, S. Taccheo, S. Longhi, O. Svelto, and C. Svelto, Opt. Mater. **11,** 269 (1999).
3. S. Taccheo, G. Sorbello, P. Laporta, G. Karlsson, and F. Laurell, IEEE Photon. Technol. Lett. **13,** 19 (2001).
4. S. Feng, F. Luan, S. Li, L. Chen, B. Wang, W. Chen, L. Hu, Y. Guyot, and G. Boulon, Chin. Opt. Lett. **8,** 190 (2010).
5. Z. Pan, H. Cai, L. Meng, J. Geng, Q. Ye, Z. Fang, and R. Qu, Chin. Opt. Lett. **8,** 52 (2010).
6. J. E. Hellstrom, G. Karlsson, V. Pasiskevicius, F. Laurell, B. Denker, S. Sverchkov, B. Galagan, and L. Ivleva, Appl. Phys. B **81,** 49 (2005).
7. Y. J. Chen, Y. F. Lin, J. H. Huang, X. H. Gong, Z. D. Luo, and Y. D. Huang, Opt. Express **18,** 13700 (2010).
8. Y. J. Chen, Y. F. Lin, X. H. Gong, Q. G. Tan, Z. D. Luo, and Y. D. Huang, Appl. Phys. Lett. **89,** 241111 (2006).
9. N. A. Tolstik, S. V. Kurilchik, V. E. Kisel, N. V. Kuleshov, V. V. Maltsev, O. V. Pilipenko, E. V. Koporulina, and N. I. Leonyuk, Opt. Lett. **32,** 3233 (2007).
10. P. Wang, J. M. Dawes, P. Burns, J. A. Piper, H. Zhang, L. Zhu, and X. Meng, Opt. Mater. **19,** 383 (2002).
11. P. Wang, J. M. Dawes, P. Burns, J. A. Piper, H. J. Zhang, L. Zhu, and X. L. Meng, in *Proceedings of OSA/ASSL 2000* MB14 (2000).
12. B. Denker, B. Galagan, L. Ivleva, V. Osiko, S. Sverchkov, I. Voronina, J. E. Hellstrom, G. Karlsson, and F. Laurell, Appl. Phys. B **79,** 577 (2004).
13. J. Li, G. Xu, S. Han, J. Fan, and J. Wang, J. Cryst. Growth **311,** 4251 (2009).
14. A. A. Lagatsky, V. E. Kisel, A. E. Troshin, N. A. Tolstik, N. V. Kuleshov, N. I. Leonyuk, A. E. Zhukov, E. U. Rafailov, and W. Sibbett, Opt. Lett. **33,** 83 (2008).
15. A. Yeniay, J. Delavaux, J. Toulouse, and W. J. Minford, Appl. Opt. **39,** 1430 (2000).
16. W. Koechner, *Solid-State Laser Engineering* (Springer, New York, 2006).
17. J. J. Zayhowski and P. L. Kelley, IEEE J. Quantum Electron. **27,** 2220 (1991).
18. I. Foldvari, E. Beregi, A. Munoz, F. R. Sosa, and V. Horvath, Opt. Mater. **19,** 241 (2002).
19. Y. J. Chen, Y. F. Lin, X. H. Gong, Z. D. Luo, and Y. D. Huang, Opt. Lett. **32,** 2759 (2007).
20. I. Y. Milev, B. A. Ivanova, M. B. Danailov, and S. M. Saltiel, Appl. Phys. Lett. **64,** 1198 (1994).
21. D. T. Walton, J. Nees, and G. Mourou, Opt. Lett. **21,** 1061 (1996).
22. H. Y. Zhu, Y. J. Chen, Y. F. Lin, C. H. Huang, Y. M. Duan, Y. Wei, Y. D. Huang, and G. Zhang, Laser Phys. Lett. **2,** 111 (2011).
23. Y. H. Tsang and D. J. Binks, Appl. Phys. B **96,** 11 (2009).